Molecular friction and epitactic coupling between monolayers in supported bilayers

R. Merkel, E. Sackmann, E. Evans

Classification
Physics Abstracts
87.20Eq

Molecular friction and epitactic coupling between monolayers in supported bilayers

R. Merkel ([1]), E. Sackmann ([1]) and E. Evans ([2])

([1]) Physik Department (Biophysics Group E22), Technische Universität München, D-8046 Garching, F.R.G.
([2]) Departments of Pathology and Physics, University of British Columbia, Vancouver, B.C. Canada, V6T 1W5

(*Reçu le 2 février 1989, accepté le 8 mars 1989*)

Résumé. — On présente des résultats expérimentaux pour la diffusion latérale de lipides fluorescents dans des bicouches déposées sur des substrats vitreux. A l'aide d'une récente théorie phénoménologique pour la diffusion sur un substrat de membrane couplée (Evans et Sackmann, 1988), on détermine la friction moléculaire intrinsèque entre les deux couches qui forment la bicouche et entre la bicouche et le substrat. On mesure les coefficients de friction entre les couches en fixant la couche mononucléaire proximale sur le substrat par des liaisons Si-O (en utilisant des silanes) ou par des ponts ioniques (arachidate de cadmium). On trouve un coefficient de friction (= rapport entre force de cisaillement et vitesse instantanée) entre deux monocouches de fluide (DMPC dans le silane) b_s égal à 3×10^5 dyne s/cm^3 et entre le fluide et la monocouche solide (DOPC sur arachidate de Cd) égal à 5×10^7 dyne s/cm^3. Dans le premier cas, b_s augmente avec le degré d'interdigitation entre les chaînes d'hydrocarbure. Afin d'étudier la friction entre la bicouche et le substrat, cette dernière est bombardée par de l'argon, ce qui provoque la séparation du substrat et de la monocouche par un film d'eau lubrifiant ultrafin (épaisseur de l'ordre du nm). On trouve un coefficient de friction entre la bicouche et le substrat $b_s = 6 \times 10^4$ dyne s/cm^3, d'où on déduit une épaisseur du film d'eau égale à 10 Å. Le second aspect de cette étude concerne les transitions de phase et le couplage monocouche-monocouche. Des bicouches symétriques séparées du substrat par un film d'eau présentent des transitions de phase abruptes à peu près à la même température que des bicouches libres (vésicules). La température de transition de bicouches asymétriques se trouve entre les valeurs correspondant à chacune des composantes. Les bicouches formées de phospholipides dans les silanes présentent une transition de phase continue à cause des contraintes imposées par une surface totale fixée. En perturbant les monocouches par l'adjonction de marqueurs fluorescents (NBD et Texas Red), on démontre que la couche proximale dans un solide ou dans un état de coexistence fluide-solide induit une transition de phase dans la couche distale (par exemple, DMPC) même si elle est déposée à partir de l'état fluide. Les monocouches de lipides insaturés sous forme cristalline compacte peuvent subir une transition de phase indépendante.

Abstract. — Microfluorescence methods were used to examine monolayer-monolayer and bilayer-substrate coupling in bilayers deposited on glass substrates. In the first part, lateral diffusion of lipid probes in individual lipid layers was measured by the fluorescence recovery after photobleach technique. The aim was to evaluate viscous molecular friction (i) between

monolayers that form a single bilayer and (ii) between a bilayer and an adjacent substrate based on a recent phenomenological theory for particle mobility in substrate-coupled membranes (Evans and Sackmann, *J. Fluid Mech.* **194** (1988) 553 [1]). To obtain coefficients for friction between monolayers, a bilayer was formed with the first (proximal) monolayer fixed to the glass substrate by Si-O-bonds (using silanes) or by ion bridges (using cadmium arachidate) ; then, probe diffusion was measured in the second (distal) monolayer formed by phospholipids. The coefficient for viscous friction (defined by b_s-interfacial shear stress/interfacial « slip » velocity) between monolayers with fluid chains (DMPC or DOPC on silane) was calculated to be in the range $b_s = 10^6$-10^7 dyn-sec/cm^3 ; between a fluid and a solid monolayer (DOPC on Cd-arachidate), the frictional coefficient was much larger, i.e. $b_s = 1\text{-}5 \times 10^8$ dyn-sec/cm^3. For two opposing monolayers with liquid chains, it was found that b_s increased with the degree of interdigitation between the hydrocarbon chains. To investigate the effect of lubrication by a water film between a fluid bilayer and the substrate, the substrate was first Argon sputtered which acted to separate the proximal monolayer from the substrate by a thin lubricating water film (thickness in nm region). The frictional coefficient between the bilayer and the substrate was measured to be in the range $b_s = 2 \times 10^3$-3×10^5 dyn-sec/cm^3 which implied that the film thickness was from 1-50 nm. In the second part, we studied the effect of monolayer-monolayer and bilayer-substrate coupling on the acyl-chain crystallization transitions in monolayers of supported bilayers. Symmetric bilayers (separated from the substrate by a water film) exhibited sharp phase transitions at about the same transition temperature as the free bilayers. The transition temperature for asymmetric bilayers was between the transition temperatures for the individual monolayer components. Bilayers formed by phospholipid monolayers on silanes showed a concerted but continuous phase transition which appeared to be due to the constraint of fixed total area and interdigitation of the two monoalayers. By doping the monolayers with different fluorescent probes (NBD and Texas Red lipid analogs), it was demonstrated that, when the proximal layer was in a solid or liquid-solid coexistence state, a phase transition was induced in the superficial monolayer even if this layer was deposited from the fluid state. It was also observed that the patterns of fluid and solid domains in both layers were in complete register. On the other hand, a fluid monolayer of unsaturated lipids on *tightly*-packed crystalline proximal monolayer was able to undergo a separate phase transition.

1. Introduction.

Stable lipid bilayers supported on solid substrates are of practical and scientific interest. Examples of practical applications are the development of biosensors [2, 3] and the simulation of cell surfaces [4]. From the scientific point of view, lipid bilayers on solids become of growing interest because of new opportunities to study fundamental properties of symmetric and asymmetric bilayers ; in particular since this arrangement facilitates the application of surface-sensitive optical techniques such as ellipsometry or evanescent-field fluorescence microscopy. Application of these techniques was made possible when it was discovered that a bilayer could be separated from the glass substrate (by a thin — many nm thick — water film) following sputtering of the substrate in an argon atmosphere [5].

The present study was organized into two parts both designed to examine monolayer-monolayer and bilayer-substrate coupling. In the first part, lateral diffusion coefficients of fluorescent probes were measured by fluorescence after photobleach-recovery methods in supported bilayers. This first aspect was motivated by a recent fluid mechanical theory [1] for particle mobility in substrate-coupled membranes where it was shown that molecular diffusivity in the membrane can be strongly affected by drag exerted at an interface (represented by a phenomenological coefficient for viscous friction). In order to derive interfacial friction coefficients, comparative measurements of probe diffusion were made in two types of substrate-coupled bilayers. In the first type bilayer, the monolayer adjacent to

the substrate (referred to as the proximal layer) was fixed to the substrate either by covalent linkage with silanes or by salt bridges with cadmium arachidate. In the second type of bilayer, the proximal layer was separated from the substrate by a thin lubricating water film. The water gap was produced by an electrostatic disjoining pressure which was created by first charging the substrate through Argon sputtering. For both types of bilayers, the outer monolayer (referred to as distal in the following) was made-up of phospholipids. With the first type of bilayer assembly, measurements of probe diffusivity in the distal monolayer yielded estimates of viscous coefficients characterizing the molecular friction between monolayers. With the second type of bilayer arrangement, measurements of probe diffusivity were used to measure frictional coefficients between the membrane and substrate (or between molecules in the proximal layer and the substrate respectively). This analysis was also used to estimate the water gap thickness.

In the second part of this work, properties of phase transitions in substrate-coupled lipid bilayers were examined. Similiar to the above studies of interfacial friction both types of bilayer configurations were employed. Observations of pronounced changes in diffusion coefficient were used to identify fluid-solid phase changes (i.e. acyl-chain conformational transitions) as a function of temperature. In addition to these measurements of probe diffusivity, static observations of fluorescence patterns were used to evaluate the microscopic organization of fluid-solid coexistence patterns (due to non-homogeneous partitioning of the fluorescent probe into fluid and solid domains). In order to evaluate coupling effects between monolayers and between bilayers and substrates, respectively the two types of bilayers described above (with fixed and decoupled proximal leaflets) were assembled. The coupling of fluid-solid coexistence patterns between monolayers was evaluated by doping the two opposing monomolecular leaflets with different types of fluorescent probes.

2. Materials and methods.

2.1 LIPIDS ([1]). — Phospholipds - L-α-dilauroylphosphatidylethanolamine (DLPE), L-α-dimyristoylphosphatidylcholine (DMPC), L-α-dimyristoylphosphatidylethanolamine (DMPE), l-α-dioleylphosphatidylcholine (DOPC) — were obtained as commercial products and used as purchased. The trichlorosilanes with hexadecyl (HTS) and octadecyl (OTS) chains were products of Petrarch System Inc. (Pristol, Penn. U.S.A.). The fluorescent probes — synthetic posphatidylethanolamines of various chain structures (DPPE, DMPE & DOPE) with 7-nitro-benz-2-oxa-1,3 diazol-4-yl (abbreviated as NBD ([1])) attached to the head groups — were purchased from Avanti Polar Lipids (Birmingham Alabama). DMPE labelled at the head group with Texas Red was synthesized in this laboratory following the procedure of Gaub (unpublished).

([1]) The following abbreviations and denominations are used :

DMPC : L-α-dimyristoylphosphatidylcholine
DMPE : L-α-dimyristoylphosphatidylethanolamine
DPPE : L-α-dipalmitoylphosphatidylcholine
DOPC : L-α-dioleylphosphatidylethanolamine
HTS : hexadeyltrichlorosilane
OTS : octadeyltrichlorosilane
NBD : 7-nitrobenz-2-oxa-1,3 diazol-4-yl
proximal : expression used for monolayer in contact with substrate
distal : monolayer in contact with semiinfinite bathing fluid
π_d, π_m : transfer pressures of distal and proximal monolayer.

2.2 PURIFICATION AND PREPARATION OF GLASS SUBSTRATES. — All substrates were carefully cleaned before use by the following procedure : stored in Millipore water for several days ; sonified in cuvette cleaner in a bath sonifier for 45 min ; Rinsed 20 times with Millipore water ; ultrasonified in Millipor water ; rinsed 20 times with Millipore water ; ultrasonified in methanol ; dried in a microwave oven. If required prior to the monolayer transfer, the glass plates were sputtered in an Argon atmosphere (99.996 % purity) which was performed in a plasma cleaner (Harric PDC-3XG).

2.3 SILANIZATION OF THE GLASS SUBSTRATES (COVERGLASSES OF $25 \times 25 \times 0.1$ mm^3). — The procedure of Nagiv *et al.* [6] was used. Clean, non-sputtered coverglass-plates were dipped into a 0.1 vol. % solution of silane in a solvent consisting of 80 vol. % n-hexadecane, 8 vol. % chloroform and 12 vol. % tetrachlorocarbon. The plates were left for 1.5 min (except for one case of only 0.5 min) in the solution. Longer incubation led to multiple layers of silane on the substrate. Surplus silane was washed-off the substrate by rinsing with chloroform. In one case, the substrate was subsequently annealed at 250 °C for 14 hours.

2.4 BILAYER DEPOSITION AND SAMPLE PREPARATION. — A film balance (described previously, cf. [7]) was used for monolayer transfer. To deposit the first (*proximal*) monolayer, the coverglass-substrate was pulled out of the aqueous phase through a surface monolayer kept at constant (proximal) pressure π_p at a pulling speed of 3.5 mm/min. During this process monolayer pressure was held constant by electronic feedback-control of film area. To deposit the second (*distal*) monolayer, the procedure of McConnell and Tamm [8] was applied. The monolayer covered substrate was carefully placed onto the monolayer deposited onto the film balance which was set at a preselected pressure (transfer pressure π_d of distal monolayer). Then, the substrate was rapidly pressed through the surface monolayer into the water subphase. In preparation for the assembly of the measuring cell a microslide with a shallow well (spherical cap-shaped, diameter 16 mm, depth 1 mm) has been placed in the aqueous subphase. The bilayer-coated coverglass was placed (below water) on the microslide with the deposited bilayer facing the well. The water subphase was aspirated out of the film balance ; residual water on the sandwiched glass plates was removed ; and then the coverglass was sealed to the slide with nail varnish.

2.5 PHOTOBLEACH-RECOVERY EXPERIMENT. — Fluorescence recovery after photobleach experiments (FRAP) were performed with a specially configured fluorescence microscope (derived from a Zeiss Axiomat microscope [9]). The beam of an Argon Ion Laser (Spectra Physics 2020-05) was divided into bleach and observation beams. The intensity of the latter was attenuated to less than 10^{-3} x the intensity of the bleach beam. This was achieved by proper positioning of two semitransparent univers with 10 % reflectivity and a neutral density filter. Both beams were focussed by the microscope objective (an oil immersion Zeiss Planapo Ph3 100 x oil) at the same spot on the surface of the bilayer-covered substrate. A computer-controlled shutter allowed rapid switching between observation and bleach beams. A set of interference filters and a dichroic mirror allowed only fluorescence emitted from the surface to pass to the Photomultiplier (RCA 31034-04). For visual observation, fluorescent light was diverted by a removable mirror to a SIT camera (Hamamatsu Photonics, C1000, Type 12). The spot bleaching technique was used to facilitate local measurement of lateral diffusivity in order to detect variations introduced by inhomogeneities in the fluorescent lipid layer. To achieve the pattern, only the central part of the laser beam was focused onto the sample by placing an aperture (0.4 mm inner diameter) in the intermediate image plane of the microscope. With this approach, a rectangular intensity profile for the bleach and observation beams was achieved.

Prior to the diffusion measurement, the beam focus was controlled with the SIT camera. Then, the prebleach fluorescence light excited by the observation beam was guided to the photomultiplier. For the initial bleach, the bleach beam was pulsed-on for a short time interval t_{B1} which was set to be smaller than 0.1 times the half-time of the fluorescence recovery $t_{1/2}$. To avoid photobleaching (during observations of fluorescence recovery), the observation beam was switched-on for only 24 short time intervals Δt_{OB} where Δt_{OB} was chosen to be $< 0.1\, t_{1/2}$. The count rate of the photomultiplier was recorded during these intervals. The total measurement time could be varied from 5 seconds to 3 hours. The values of lateral diffusivity D were derived from the half-time of fluorescence recovery $t_{1/2}$ with the following relation :

$$D = 0.224\, r^2/t_{1/2}$$

where r is the radius of the bleach spot (usually $r = 9$ μm) and $t_{1/2}$ is the fluorescence recovery half-time defined as by Axelrod *et al.* [10]. The glass sample plates were fixed onto a copper heat exchange stage and the objective was surrounded by a heat exchange collar. The temperature of the sample was controlled by a water bath. This ensured a constant equilibrium temperature of the immersion oil between the objective and the sample and thus a constant temperature of the bilayer-substrate assembly. Temperature was measured with thermistors, one on top of the microslide and one on the copper stage.

3. Lateral diffusion measurements and apparent phase transitions.

3.1 DIFFUSION IN SUPPORTED DMPC-BILAYERS *VERSUS* TEMPERATURE. — Figure 1 presents the results for probe diffusion measured as a function of temperature in a symmetric supported bilayer of DMPC (on sputtered glass) with the fluorescent probe (NBD-DMPE) in the distal monolayer. The monolayers were transferred at different pressures (17.2 dyn/cm for the proximal layer and 29.7 dyn/cm for the distal monolayer). The significant features in figure 1 are recognized as :

(i) the supported bilayer clearly exhibited a liquid crystal-to solid transition at a temperature ($T_t = 20$ °C) slightly lower than the chain melting transition temperature of free bilayers in DMPC vesicles ($T_t = 24$ °C) ;

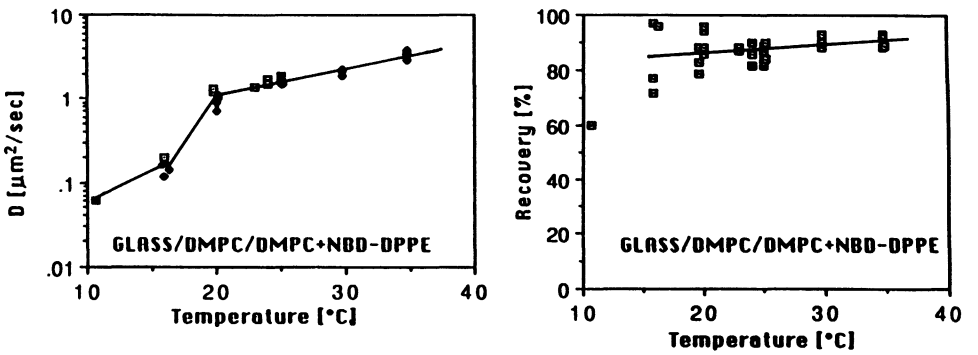

Fig. 1. — Left : temperature dependence of the diffusion coefficient, D (on a logarithmic scale), of the NBD-DMPE probe in the distal layer of a supported bilayer of DMPC. Transfer pressures of distal film 30 mN/m and and of proximal 17 mN/m. The transfer was performed at 25 °C. Several measurements (indicated by the squares) are given for each temperature which show the variance of the measurement. Right : corresponding temperature plot of the degree of fluorescence recovery, R. Again several measured values are given for each temperature. The straight lines are only drawn to guide the eye.

(ii) above T_t, log D increased linearly with temperature where the slope $\mathrm{d}\ln(D)/\mathrm{d}(1/T) = (6.5 \pm 1.0) \times 10^3$ K was somewhat larger than that found for isolated DMPC bilayers, i.e. $(3.5 \pm 0.5) \times 10^3$ K [11, 12].

Note : this slope corresponds to an apparent activation energy of $\Delta E_{app} = (54 \pm 10)$ kJ/M whereas that for free DMPC bilayers was found to be $\Delta E_{app} = 2(9 \pm 5)$ kJ/M [12] ;

(iii) the value of D at temperature well-below T_t (at 10 °C) was $D = 0.05$ μm^2/sec which was much higher than the value characteristic for the L_β phase of bilayers ($D < 10^{-3}$ μm^2/sec). This point will be discussed later in terms of defect structures in supported bilayers.

In another experiment, the diffusion coefficient was determined in symmetric DMPC bilayers where *both* layers were formed at 20.0 dyn/cm. In this experiment, measurements of probe (NBD-DMPE) diffusion were made separately in both distal and proximal layers. At a temperature of 25 °C, the diffusion coefficient was found to be $D = 1.\ (30 \pm 20)$ μm^2/sec in the distal layer and $D = 1.\ (26 \pm 20)$ μm^2/sec in the proximal layer, i.e. equivalent within experimental error. This result demonstrated that the monolayers were strongly coupled vis a vis the weak interaction with the substrate (across the lubricating film of water).

3.2 DIFFUSION IN DISTAL (SUPERFICIAL) MONOLAYERS ON SUBSTRATE-FIXED MONOLAYERS OF VARIABLE PACKING DENSITY. — In figures 2 and 3, results are presented for measurements of probe diffusivity in DOPC and DMPC monolayers deposited on several types of proximal monolayers which were fixed to the substrate.

Figure 2 summarizes data for the case of a distal DOPC monolayer with NBD-DOPE as molecular probe. The pertinent features apparent in figure 2 are

(i) breaks or abrupt changes in the *D-versus-T* plots were observed in all cases. These provided evidences for weak conformational changes in all cases which were associated with substantial reductions in the probe mobilities with decreasing temperature (see also [13]). These reductions were, however, much smaller than in case of the chain crystallization of DMPC bilayers (cf. Fig. 1). Comparison of figures 2a to 2d shows that the conformational changes started at about the same temperature (25 °C) in all cases suggesting that it is a characteristic feature of the DOPC-lipid ;

(ii) in all tests of figure 2 the fluorescence recoveries were high (> 80 %) and were essentially constant over the whole temperature range and are therefore not shown. This suggests that the DOPC monolayer was in a fluid-like state at all temperatures (both above and below the conformational change) and/or that the solidified islands formed at the transitions were much smaller than the bleach spot diameter ;

(iii) the mobility of the probe appeared to decrease with increasing chain length of the silanes above the conformational transitions (cf. Figs. 2a to 2c). The diffusivity of DOPC on the Cd-arachidate monolayer was much smaller than on the silanised substrates indicating that D decreases with increasing packing density of the proximal monolayer. (Note that an increase in packing density reduces the chain mobility).

In figure 3, the results for DMPC (with an NBD-DMPE probe) above hexadecyltrichlorosilane (HTS) are shown. Conformational transitions (apparent as changes in diffusivity) were again found in distal DMPC monolayers. The reduction in lateral mobility across the apparent transition was much less than that observed for symmetric DMPC bilayers separated from the substrate by a lubricating water film (Fig. 1). To evaluate the influence of the packing density on probe diffusivity in the distal monolayer, both the transfer pressure of the distal DMPC-monolayer and the surface density of the proximal silane film were varied. The latter was

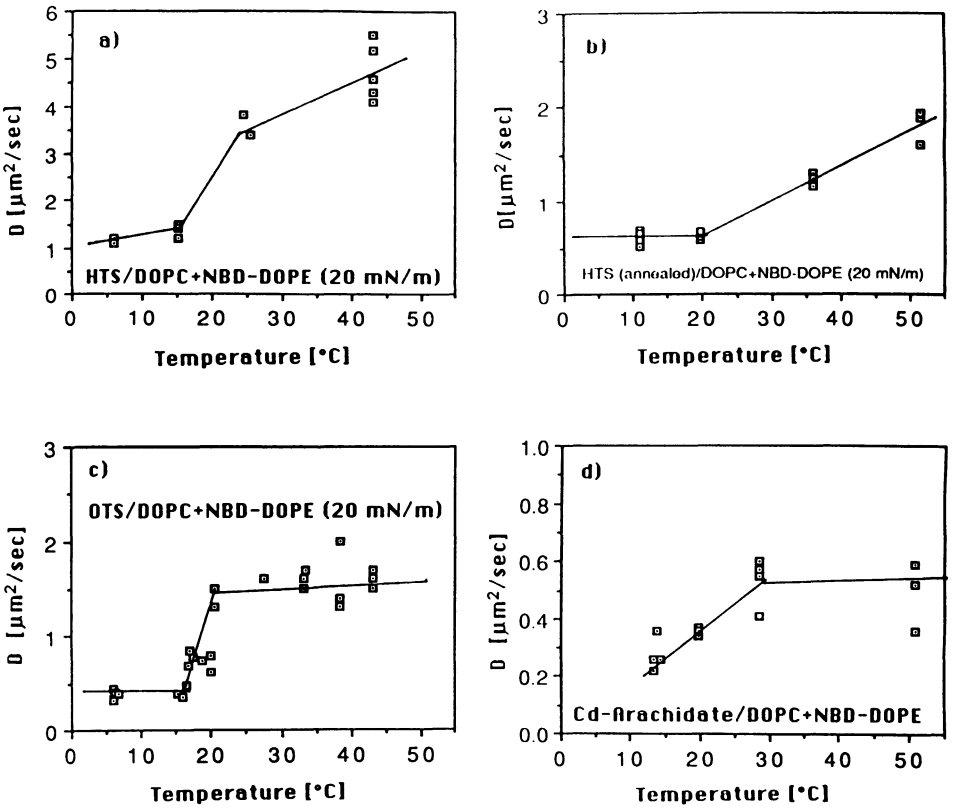

Fig. 2. — Temperature dependence of the diffusion coefficient of NBD-DOPE in DOPC-monolayers on monomolecular films which are fixed to the substrate. a) Hexadecyltrichlorosilane (HTS) deposited from solution for 1.5 min. b) Same as in a), but after annealing of the silane layer at 250 °C for 14 hs. c) Octadecyltrichlorosilane (OTS) deposited from solution for 1.5 min. d) Cadmium arachidate deposited at a pressure of 30 mN/m. DOPC was in all cases deposited at 20 mN/m and 25 °C.

accomplished through reduction of the time for adsorption in the silane solution from 1.5 to 0.5 min (cf. Fig. 3d). The significant features apparent in figure 3 (and related experiments, not shown) are as follows :

(i) in all cases, broad conformational transitions were indicated by major reductions in lateral mobility of probes as the temperature was lowered ;

(ii) the nature of these transitions depended critically on the relative packing densities of the two layers. The change in diffusivity was comparatively sharp in the case of figure 3b where DMPC had been transferred at a pressure of 20 dyn/cm. However for other cases where DMPC had been transferred at higher (31.4 dyn/cm, Fig. 3a) and lower (10 dyn/cm, Fig. 3c) pressures, the diffusion coefficients showed more continuous transitions ;

(iii) the fluorescence recovery also showed a sharp drop in the case of DMPC transferred at 20 dyn/cm (Fig. 3b) but remained essentially constant for the cases where transitions were continuous. These results showed that coupling between monolayers of the bilayers was quite different for each case ;

(iv) comparison of figure 3d and 3c shows a surprising result. For the (supposedly) less-densely packed HTS film (Fig. 3d), the diffusion coefficient decreased much faster with

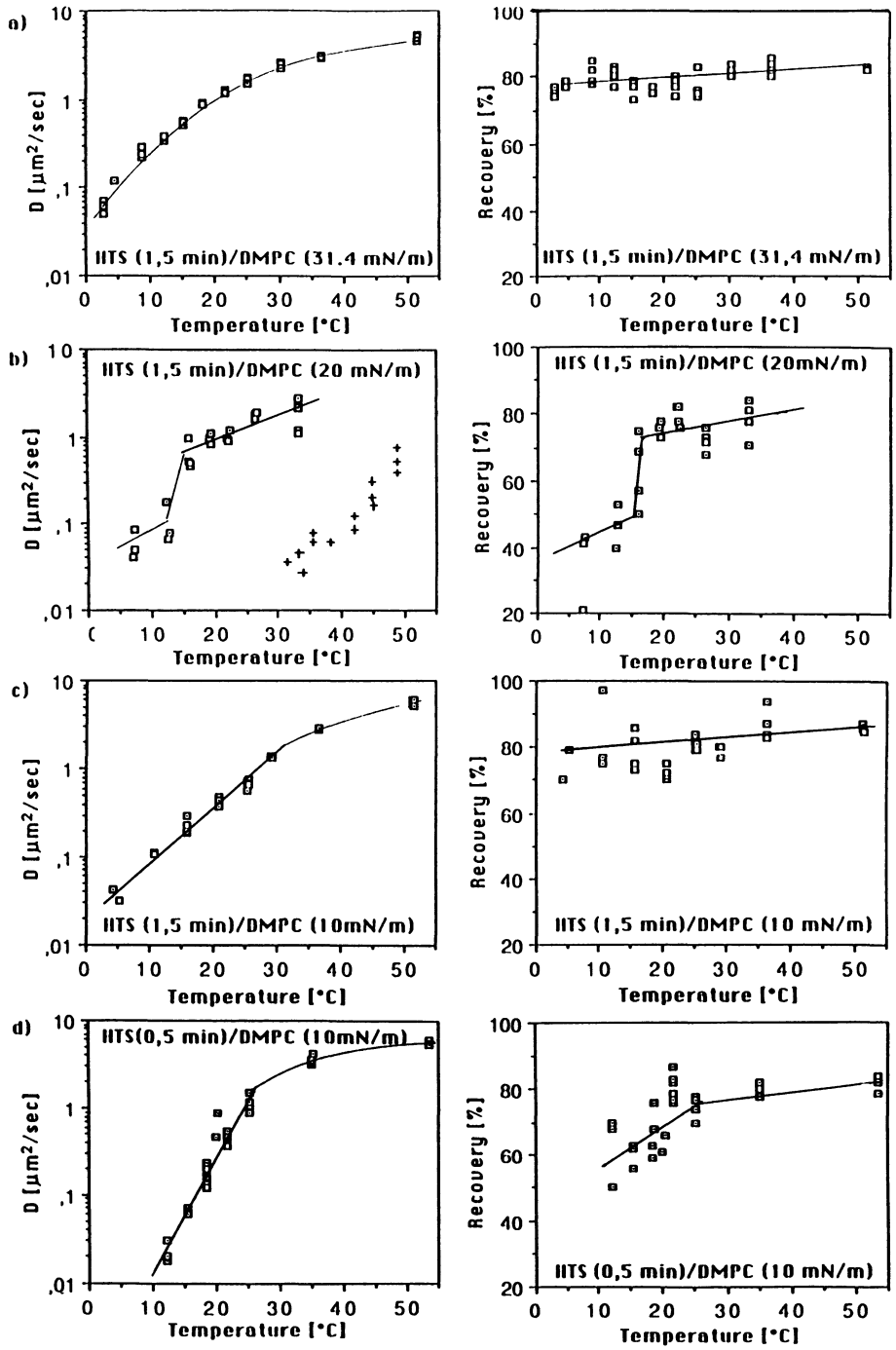

Fig. 3. — Temperature dependence of the diffusion coefficients, D, (left side) and fluorescence recoveries, R (right side) of NBD-DMPE in DMPC monolayers swimming on hexadecyltrichlorosilane (HTS) monomolecular layers. a to c : HTS-layer deposited from solution (with 1.5 min equilibration-time) with DMPC transferred from 31.4 mN/m (a), 20 mN/m (b) and 10 mN/m (c). HTS layer deposited from solution with only 0.5 min of equilibration and distal DMPC layer transferred at 10 mN/m (d). The crosses in figure 3b are the diffusion coefficients for DMPC transferred at 20 mN/m on OTS.

decreasing temperature than for the case of the tightly packed HTS film (Fig. 3c). Again, the packing density of the silane film was assumed to increase with increasing time for adsorption to the glass in the silanising solution ;

(v) by comparison, the conformational change in a DMPC monolayer deposited on an OTS layer appeared to occur at a much higher temperature (cf. curve added to Fig. 3b) ;

(vi) a continuous transition was also observed in the case of DMPC (transferred from 20 dyn/cm) on to a 1 : 1 mixture of HTS and OTS.

As will be discussed in the next section, kinetic models indicate that the diffusion coefficient in free bilayers should decrease exponentially with increasing surface density. However for substrate-coupled bilayers, frictional effects at monolayer-monolayer and bilayer-substrate interfaces are also expected to be affected by packing density and monolayer pressure ; if sufficiently strong, frictional effects may dominate the diffusivity. Thus, systematic measurements of the diffusion coefficient as a function of the transfer pressure were carried out to distinguish intrinsic monolayer packing density effects from intermonolayer friction, to evaluate the influence of lipid packing density on interlamellar friction, and to test whether changes in packing density occurred during monolayer transfer.

3.3 EFFECT OF TRANSFER PRESSURE ON DIFFUSIVITY. — Additional measurements for symmetric DLPE bilayers in figure 4a show how the diffusion coefficient in the proximal layer was effected by its transfer pressure whereas data in figure 4b show the influence of transfer pressure in the distal monolayer on diffusivity. The results demonstrate the following important features :

(i) probe diffusion in the proximal layer (Fig. 4a) decreased with increasing transfer pressure which indicated that no drastic alteration in the surface density occurred during monolayer transfer. However, the increase in diffusivity with decreasing transfer pressure was much less than expected from the molecular « free » volume model (discussed in the next section). This discrepancy plus the large reduction observed for probe mobility (compared to free bilayers) suggested that a frictional effect was present which depended on packing density. (Note : the measured value of $d(D)/d(\pi) \approx -11\ \mu m^2$ sec/kg, whereas the free volume model predicts $d(D)/d(M) < -22\ \mu m^2$ sec/kg) ;

(ii) the unexpected result was that probe diffusivity in the distal monolayer (Fig. 4b) increased with increasing transfer pressure ;

(iii) for fixed transfer pressure in the distal layer, probe diffusivity in the distal layer decreased when the transfer pressure was lowered for the proximal layer (compare data in Fig. 4b).

It should be noted that the diffusion coefficients in the test of figure 4 were measured at two temperatures : 25 °C and 35 °C. The measured D values in the proximal layer exhibited a larger variance at 25 °C than at 35 °C. However, at all temperatures the diffusion coefficients of probes in the proximal monolayer were about equal to or rather larger than in the distal monolayer. We therefore conclude that both monolayers are strongly coupled together but are separated from the glass surface by a water layer.

3.4 THEORETICAL ASPECTS OF DIFFUSION.

3.4.1 *Membrane-substrate frictional effects.* — The experiments just described were motivated by a recent analysis [1] of particle mobility in a liquid membrane coupled to a rigid substrate. The development was an extension of the phenomenological theory for diffusion in free liquid membranes introduced by Saffman and Delbruck [14] and further analyzed by Hughes *et al.*

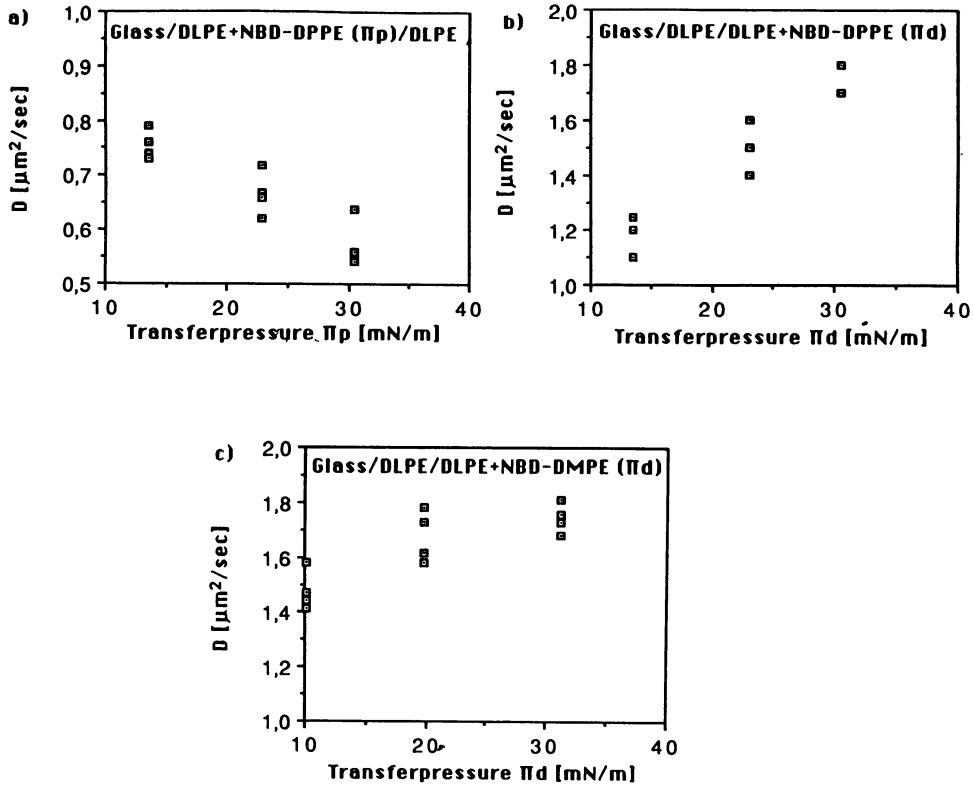

Fig. 4. — Effect of the variation of the transfer pressures of proximal and distal monolayer on its diffusion coefficient for the case of supported bilayers of DLPE. a) Dependence of the diffusion coefficient in the proximal monolayer on its transfer pressure in all cases measured at 25 °C. The distal DLPE layer is deposited from 17.6 mN/m, b and c) Dependence of the diffusion coefficient in the outer monolayer on its transfer pressure for two values (17.5 mN/m (b) and 20 mN/m (c)) of deposition pressure of the proximal monolayer (Diffusion measured at 35° C).

[15]. For the substrate-coupled membrane (cf. Fig. 5), the transfer of momentum from the membrane flow field (created by particle motion) to the third dimension is dominated by the presence of the substrate at large distances from the particle. For a particle of radius a_p (which spans the membrane) moving with instantaneous surface velocity v_p, particle drag is produced by two effects, i.e. $F_D = (\lambda_m + \lambda_p) v_p$. The first term accounts for the viscous dissipation in the membrane plus friction between the fluid membrane and the substrate whereas the second term is the direct friction between the probe and the rigid surface ; λ_m and λ_p are the corresponding drag coefficients in dyne-sec/cm. According to kinetic theory, the diffusion coefficient D is determined through the Einstein relation, $D = kT/(\lambda_m + \lambda_p)$. To determine the drag created by membrane flow, the 2-dimensional equation of motion was solved including the effect of interfacial drag on the membrane caused by adjacent immobile substrates-or-across a lubricating liquid layer to the substrate. Interfacial friction was modeled by assuming that the interfacial shear stress σ_s was proportional to the local membrane velocity, i.e. $\sigma_s = b_s v$. For a purely lubricative layer of liquid between membrane and substrate (with thickness h_f and viscosity μ), the frictional coefficient b_s (measured in units viscosity/length) is simply μ / h_f as prescribed by the linear

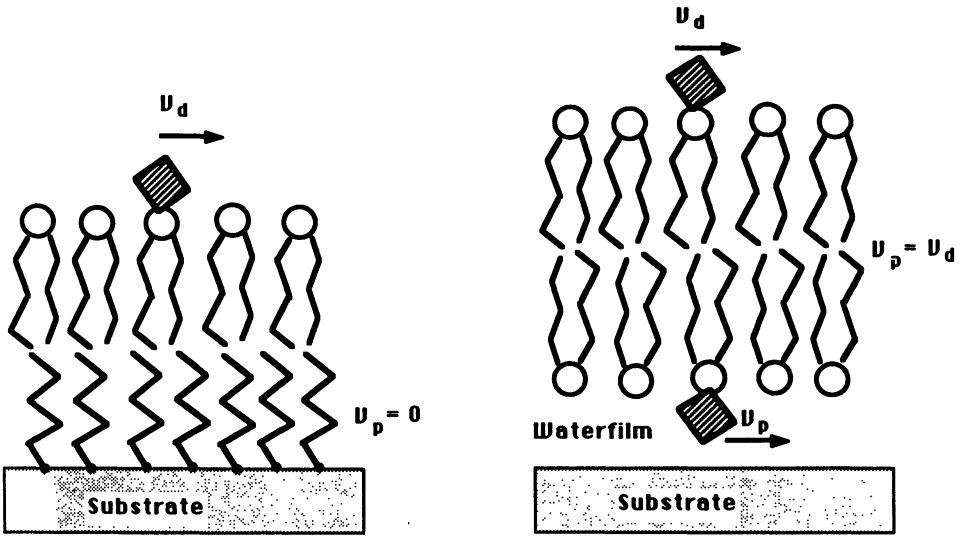

Fig. 5. — Schematic illustration of a lipid probe in the proximal or distal monolayer of a (in general asymmetric) bilayer coupled to a solid substrate. Two limiting situations are possible : tightly coupled monolayers ($\nu_d = \nu_p$) (this case is realised at lipid bilayers swimming on a thin water film) and fixed proximal monolayer $\nu_p = 0$ (realised in lipid monolayers on silane- or Cd-arachidate-covered substrates).

velocity gradient and the relation $\sigma_s = \mu\,(v/h_f)$. For direct frictional interactions (e.g. between monolayers or between monolayer and substrate), the liquid continuum model for shear stress across a lubricating layer is replaced by the phenomenological proportionality of $b_s = \sigma_s/v$; b_s becomes an intrinsic property of the interface. With this model for interfacial friction, the particle drag coefficient λ_m for membrane flow was found to be given by membrane surface viscosity times a universal function $f(\varepsilon)$ of the dimensionless particle radius [1].

$$\lambda_m = 4\,\pi\eta_m\left[\frac{1}{4}\,\varepsilon^2 + \varepsilon\,\frac{K_1(\varepsilon)}{K_0(\varepsilon)}\right] \tag{1}$$

where $\eta_m = \eta_{B1}$ is the intrinsic 2-D-viscosity of the free bilayer (or $\eta_m = \eta_{B1}/2$ for a monolayer) in an infinite aqueous medium ; K_0 and K_1 are modified Bessel functions of zero and first order ; the argument ε is the dimensionless particle radius given by $\varepsilon = a_p(b_s/\eta_m)^{1/2}$ where $\eta_m = \eta_{B1}$ or $\eta_m = \eta_{B1}/2$ as required. It should be noted that membrane surface viscosity η_m is formally equivalent to a 3-D viscosity μ_m times the membrane thickness h_m (i.e. $\eta_m = \mu_m h_m$). Similarly, it was anticipated that the probe may exhibit a separate « self-drag » characteristic for interaction with the substrate. Hence, another continuum approximation was introduced into the analysis to represent particle-substrate friction, i.e. $F_p = \pi a_p^2 b_p v_p$. Therefore, the ε^2 term in the universal function $f(\varepsilon)$ is simply augmented by a factor $(1 + b_p/b_s)$ to include this possibility. Since the diffusing particle (probe) is often an analogue of membrane constituents, the ratio b_p/b_s can be taken as approximately unity.

Additional drag due to an exterior bathing solution above the membrane is not large and can be treated with a simple approximation. Here, the dimensionless particle radius ε is modified to include an additional friction coefficient b_∞ which represents the exterior

fluid phase above the bilayer, i.e. $\varepsilon = a_p[(b_s + b_\infty)/\eta_m]^{1/2}$. It was found that the effect of the semi-infinite bathing fluid adjacent to the membrane is well-approximated by

$$b_\infty = 2\,\mu_\infty^2/\eta_{B1} = \mu_\infty/\delta \tag{2}$$

where μ_∞ is the 3-D viscosity of the exterior aqueous phase and where δ is a length which characterizes the penetration of the membrane flow field into the third dimension ($\delta = \eta_{B1}/2\,\mu_\infty$)

$$\varepsilon = a_p[(b_s + 2\,\mu_\infty^2/\eta_{B1})/\eta_m]^{1/2} \tag{3}$$

or equivalently,

$$\varepsilon = \varepsilon_\infty[b_s\,\eta_{B1}^2/4\,\mu_\infty^2\,\eta_m + \eta_{B1}/2\,\eta_m]^{1/2} \tag{4}$$

where $\varepsilon_\infty = 2\,a_p\,\mu_\infty/\eta_{B1}$ is the dimensionless particle radius for probe motion in a free bilayer. Again, the surface viscosity η_m is to be chosen as η_{B1} or $\eta_{B1}/2$ appropriate to the particular membrane-substrate assembly.

Let us consider now two cases.

1) When the probe is moving in the distal monolayer adjacent to a fixed proximal monolayer, then $\eta_m = \eta_{B1}/2$ and the dimensionless particle radius (to be used in the drag coefficient equation) becomes,

$$\varepsilon_{M1} = \varepsilon_\infty[1 + b_s(\eta_{B1}/2\,\mu_\infty^2)]^{1/2} = \varepsilon_\infty[1 + b_s\,a_p/\varepsilon_\infty\,\mu_\infty]^{1/2}\,. \tag{5}$$

2) When the probe is moving in either monolayer of a bilayer *weakly* coupled to the substrate (e.g. by a thin lubricating film of water), then intermonolayer friction strongly couples the probe motion in one monolayer to the adjacent monolayer as if the probe was a transbilayer particle. Consequently, the dimensionless particle radius is specified with $\eta_m = \eta_{B1}$

$$\varepsilon_{B1} = \varepsilon_\infty[(1 + b_s\,a_p/\varepsilon_\infty\,\mu_\infty)/2]^{1/2}\,. \tag{6}$$

For a lubricating water film of thickness h_f, $b_s = \mu_\infty/h_f$ and we obtain

$$\varepsilon_{B1} = \varepsilon_\infty[(1 + \delta/h_f)/2]^{1/2}\,. \tag{7}$$

This equation is valid for $h_f \ll \delta$ and has the obvious self-consistent limit $\varepsilon_{B1} = \varepsilon_\infty$ for $h_f = \delta$.

In order to determine frictional properties of substrate-coupled membranes, the following procedure is required. The first step is to establish the intrinsic viscous properties of the constituents as a free bilayer. This establishes the surface viscosity η_{B1} and (with the particle size a_p) the value of the dimensionless particle radius ε_∞ for the free bilayer which are the parameters required in the particle drag relations. Clearly, the surface viscosity η_m (and thus ε_∞) depend on temperature and surface density which also must be established *a priori*. Hence, probe diffusivity is measured in free bilayers as a function of temperature (surface density is uniquely determined by temperature for a free bilayer in a large aqueous phase). Using the fluid mechanical relation for drag coefficient (reciprocal of mobility) and the Einstein kinetic equation for diffusivity, measurements of lateral diffusion in free bilayers are converted to values of η_m and ε_∞.

The next step is to measure probe diffusivity in substrate-coupled layers where the state of the monolayer in which the probe diffuses is equivalent to a surface density state for a free

bilayer system. In this case, the surface viscosity and prefactor ε_∞ are taken from the values determined for the free bilayer. To derive estimates of viscous coefficients for interfacial friction, the appropriate relation for dimensionless particle radius is chosen (either ε_{B1} or ε_{M1} as described previously) which represents the bilayer-substrate assembly process ; then, the universal drag relation $f(\varepsilon)$ is used to convert the measured value of diffusivity (arranged as $4\ \pi\ D\eta_m/kT$) to the corresponding value of the phenomenological coefficient b_s.

3.4.2 *Temperature and monolayer packing effects.* — The variation of the diffusivity in a free liquid membrane with lateral pressure can be understood in terms of a molecular « free » volume (or molecular « free » area) model which relates D to the surface density of the bilayer. The model is based on the Cohen-Turnbull model for diffusion in glasses which was extended to fluid membranes [11]. The model predicts that the sensitive temperature dependence of the diffusion coefficient in fluid bilayers is due to changes in « free » volume caused by bilayer thermal expansion in contrast to a rate-reaction activated process. The molecular « free » volume (or area) is the excess volume (area) per molecule at a given temperature above the volume (area) for the ultimate « hard-packed » state (usually taken as the crystalline state). The model specifies that the diffusivity depends exponentially on the surface density which has been well verified by measurements in monolayers at air/water interfaces [16].

3.5 DETERMINATION OF VISCOUS COEFFICIENTS FOR INTERFACIAL FRICTION. — Two problems arise in calculations of frictional coefficients from measurements of probe diffusivity. First, the diffusion coefficient depends on two unknown parameters, i.e. the frictional coefficient b_s and the membrane surface viscosity η_m. Further, according to the predictions of the molecular « free » volume model just outlined, surface viscosity depends on surface density of the bilayer (or monolayer) which is clearly variable. The second problem concerns the assumptions employed in the fluid mechanical analysis of particle drag in substrate-coupled membranes. In the original analysis [1], the equation of motion was solved for a particle moving in a single membrane layer coupled to a rigid substrate (either directly or across a lubricating film of 3-D liquid). As such, this treatment is appropriate for probe motion in a superficial monolayer adjacent to a proximal monolayer that has been immobilized by fixation to the solid substrate, e.g. DOPC and DMPC on fixed proximal monolayers of silanes or Cd-arachidate (Figs. 2 and 3). Therefore, we have used the relation for dimensionless particle radius ε_{M1} and $\eta_m = \eta_{B1}/2$ in the prescription for drag coefficient to estimate the viscous coefficient b_s for intermonolayer friction from these data. However for supported bilayers separated from the substrate by a thin film of water (e.g. symmetric DMPC bilayers on glass), the analysis would appear to be applicable only if the probe spanned both monolayers so that the bilayer could be considered as a single layer. Even though the probe only spanned one layer, it is reasonable to treat this case as if the probe spanned both layers. The rationale is that the frictional coupling between distal and proximal monolayers *greatly* exceeds the interfacial drag of the lubricating water film on the underside of the bilayer, so the surface flow fields created by particle motion will be nearly the same in either layer. Thus, the *ad hoc* assumption is that the monolayers are strongly coupled vis a vis coupling to the substrate across the lubricating water film. This assumption is supported by the experimental observation that probe diffusion measured separately in distal and proximal monolayers of symmetric DMPC bilayers (separated from the glass substrate by a water film) was found to be the same (cf. discussion of Fig. 1). Therefore in this case, we have used the prescription for the drag coefficient with ε_{B1} as the relation for dimensionless particle radius

and $\eta_m = \eta_{B1}$ in order to derive estimates of the viscous coefficient for the lubricating water film and the film thickness.

The method of calculation described above was applied to data for DOPC and DMPC monolayers supported by fixed monolayers (Figs. 2 and 3). Here, diffusion coefficients for probes in free bilayers of synthetic lecithins [12] were used to establish η_{B1} and the prefactor ε_∞ at 45 °C. These values were expected to be the same for both DMPC and DOPC at 45 °C because Galla *et al.* [11] measured diffusion for pyrene probes in both DMPC and DOPC bilayer vesicles and found nearly the same values at 45 °C. Values for diffusivity and viscosity at lower temperatures were derived from the temperature dependence of diffusivity found for free bilayers [12]. The crucial assumption (which is implicit in the use of these values) is that monolayers transferred at 20 dyn/cm pressure represent the fluid state in free bilayers. Particle radii a_p were taken as 4 Å for DMPC and 5 Å for DOPC as estimated from the area per molecule in film balance experiments. Table I outlines the properties of free bilayers used in the calculations of viscous coefficients for interfacial friction. Table II presents measurements of probe diffusion in distal DOPC and DMPC monolayers supported by fixed proximal monolayers and the values calculated for viscous coefficient b_s which represent friction between monolayers. An additional calculation was performed. The viscous coefficient for the lubricating water film between a DMPC bilayer and sputtered glass was estimated along with the film thickness. Here, values for probe diffusion were found to be 5.7 μm^2/sec for a transfer pressure of 15 dyn/cm at 25 °C. Since precise surface densities for monolayers were not known, we have assumed that free DMPC bilayers at the same pressure would be characterized by diffusivities form 6 to 11 μm^2/sec (the range of diffusivity for free DMPC bilayers between 25 °C-45 °C). With this assumption, the viscous coefficient for interfacial drag was estimated to be between 2×10^3 and 3×10^5 dyn-sec/cm^3. Further, the drag coefficient for the lubricating water film was converted to an estimate of the film thickness h_f, i.e. 1-50 nm.

Table I. — *Kinetic and viscous properties of free bilayers.*

Lipid	T Temperature °C	D Diffusion Coefficient $\mu m^2/s$	η_m Surface Viscosity 10^{-7} dyn-s/cm	ε_∞ Dimensionless Particle Radius 10^{-3}	b_s Viscous coefficient for Interfacial Drag (1) dyn-s/cm^3
DMPC	25°	6	3.3	2.4	6.1×10^2
	45°	11	1.74	4.6	1.15×10^3
DOPC	10°	2.5	8.5	1.17	2.35×10^2
	45°	10-11	1.63-1.81	5.5-6.1	$1.23\text{-}1.10 \times 10^3$

(1) A value of $b_s = 10^3$ dyn-s/cm corresponds to a characteristic depth $\delta = 10^{-5}$ cm for penetration of the surface flow field into the exterior aqueous phase.

3.6 DISCUSSION OF DIFFUSION DATA AND CALCULATIONS OF VISCOUS PROPERTIES. — As shown in tables I and II, most measurements of probe diffusivity were characterized by dimensionless particle radii ε on the order of one or less. For values of $\varepsilon \ll 1$, the relation for particle mobility (λ_t^{-1}) depends logarithmically on the dimensionless radius. Consequently,

Table II. — *Viscous properties for interfacial drag between fluid and immobilized monolayers.*

A. Distal Layer : DOPC with NBD-DOPE probe (Transfer pressure 20 dyn/cm)

Proximal Layer Properties	D Probe Diffusivity in Distal Layer $\mu m^2/sec$	T Temperature (1) °C	b_s Viscous Coefficient for Intermonolayer Drag dyn-sec/cm^3	ε
HTS (1.5 min adsorption at 25 °C, not annealed)	1.2	10°	1×10^7	0.24
	5	45°	4.5×10^6	0.34-0.4
HTS (1.5 min adsorption at 25 °C, annealed at 250 °C)	0.6	10°	6×10^7	0.6
	1.8	45°	4.5×10^7	1.1 -1.2
OTS (1.5 min adsorption at 25 °C, not annealed)	0.4	10°	1×10^8	0.95
	1.8	45°	4.5×10^7	1.1 -1.2
Cd-arachidate (Transfer Pressure 30 dyn/cm)	0.2	10°	5×10^8	1.7
	0.58	45°	1.6×10^8	2.1-2.3

(1) Note that the values of D at 10 °C may be reduced by the formation of solid domains exhibiting diameters small compared to the bleach spot diameter (cf. reference [20]).

B. Distal Layer : DMPC with NBD-DMPE Probe (Transfer Pressure 20 dyn/cm)

Proximal Layer Properties	D Probe Diffusivity in Distal Layer $\mu m^2/s$	T Temperature °C	b_s Viscous Coefficient for Intermonolayer Drag dyn-sec/cm^3	ε
HTS (0.5 min adsorption at 25 °C, not annealed)	7	45°	2.7×10^6	0.23
HTS (1.5 min adsorption at 25 °C, not annealed)	5	45°	7×10^6	0.36
OTS (1.5 min adsorption at 25 °C, not annealed)	0.7	45°	2.9×10^8	2.3
OTS : HTS (1 : 1) (1.5 min adsorption at 25 °C, not annealed)	5	45°	7×10^6	0.36

small changes in diffusivity may represent large viscous frictional effects as given by the coefficients in table II. When $\varepsilon > 1$, the diffusivity moves to a regime where the diffusion coefficient is inversely proportional to the square of the particle radius. Obviously, certain situations represented this regime of strong dependence on probe size (e.g. DOPC on Cd-arachidate). In the derivations of viscous coefficients for interfacial friction, we have only applied the method of calculation to data for distal monolayers on fixed proximal layers where it was clear that the distal layer was in the fluid state (i.e. DMPC at 45 °C and DOPC at 10 °C and 45 °C with both sets of distal layers transferred at 20 dyn/cm pressure). In these calculations, we have used values of diffusivity for free bilayers at these temperatures with the implicit assumption that monolayer pressures of 20 dyn/cm would be appropriate to the free bilayer state (i.e. 40 dyn/cm for the free bilayer). Support for this assumption comes from comparison of pressure-area isotherms for monolayers at air-water interfaces with X-ray structure data for area per molecule in fully hydrated multibilayers [17]. Also, theoretical models [17, 18] indicate similar values for pressure in free bilayers. However, there is a considerable range in the estimates of surface pressure predicted for monolayers of free bilayers (e.g. 15-30 dyn/cm) ; thus, this assumption is not completely reliable. The best approach would be to measure probe diffusion in monolayers condensed to the appropriate pressures and densities at air-water (or other liquid-liquid) interfaces. In the analysis of fluid monolayers on fixed proximal layers, the diffusivity values chosen for the free bilayer state were not so critical because the diffusivity was drastically reduced by the presence of the fixed proximal-monolayer substrate. In any case, the coefficients b_s for viscous friction must be regarded as order of magnitude estimates. Some particular features to be noted in table II are outlined as follows :

(i) the largest coefficients for viscous friction resulted from the analysis of data for fluid monolayers adjacent to Cd-arachidate layers. It is well known that this layer was in the crystalline state thus these coefficients represent interfacial drag of a fluid monolayer relative to a solid hydrocarbon surface. As such, these coefficients are an order of magnitude greater than the value predicted by a model of a 1 nm hydrocarbon oil film with a 1 poise viscosity, i.e. $b_s \approx 10^7$ dyn-sec/cm^3 ;

(ii) values for viscous frictional coefficients derived from data for DOPC and DMPC monolayers on HTS are in a range comparable to the model of interfacial drag across a 1 nm thick layer of hydrocarbon oil ;

(iii) the remarkable result was that the viscous coefficient for interfacial friction was found to increase with the apparent extent of interdigitation between fluid chains of the distal and proximal monolayers. The evidence to support this interpretation comes from the comparison of coefficients for DOPC and DMPC on proximal layers of HTS and OTS.

In contrast with the calculation of coefficients for interfacial drag between monolayers just discussed, calculation of the viscous coefficient for friction between the proximal layer and glass substrate across a lubricating water film was much less reliable. The difficulty is that the presence of the lubricating water film significantly decoupled the bilayer from the substrate. Thus, the values measured for probe diffusivity were not reduced as much as for the situations where the proximal monolayer was immobilized by attachement to the substrate. Based on predictions of the viscous coefficient for interfacial drag across the thin water layer (i.e. $b_s < 10^6$ dyn/sec/cm^3 for $h_f > 1$ nm), it is readily apparent that probe diffusivity in the monolayers will not be greatly reduced in comparison to probe diffusion measured in free bilayers. Obviously, reduction in probe mobility will only be pronounced when the proximal layer is very close to the substrate. Because of the uncertainties in surface properties of the DMPC monolayers in bilayers separated from the glass substrate by a water film, we are only

able to estimate a broad range for the separation distance i.e. 1-50 nm. However, the resolution in this type of experiment can be greatly improved with the procedures described above for prior determination of monolayer properties at well defined surface pressures.

4. Epitactic coupling and frustrated phase transitions in supported bilayers.

4.1 INDUCED PHASE TRANSITIONS AND EPITACTIC COUPLING. — In previous electron micrograph studies [7, 9], it was found that monolayers could be transferred from an air water interface (in any condensed state, i.e. fluid-solid coexistence or solid) onto a hydrophilic substrate without significant structural changes. Data for probe diffusion in the proximal monolayer of a supported bilayer (Fig. 4a) corroborated this conclusion since the diffusion coefficient was observed to increase with decreasing lateral transfer pressure consistent with the « free » volume kinetic model. However, other results in this study imply that the phase structure of the distal monolayer was largely dictated by the structure of the proximal monolayer. In general (with the exception of DOPC on Cd-arachidate), the deposition of a fluid monolayer (e.g. DMPC or DLPE) onto a proximal layer in the crystalline state induced the distal (fluid) monolayer to solidify.

The most striking evidence of the strong coupling between monolayers was provided by the experiments presented in figure 6. Here, a monolayer of DMPE (doped with Texas Red labelled DMPE) was deposited from a fluid-solid coexistence state onto Argon sputtered glass. Then, DMPC (doped with NBD-DMPE) was deposited above the first layer at a transfer pressure (20 dyn/cm) which clearly represented an expanded fluid state. The left and right micrographs of NBD (465 nm) and Texas Red (596 nm), respectively. Independent excitation of the fluorescent probes was assured because the excitation spectra for the two labels was widely spaced in wavelength. Also, since both types of fluorescent probe were attached to head groups, the average distance between each probe type was much greater than 5 nm (the Forster radius) ; hence, energy transfer could be excluded. The dark areas formed in the DMPC monolayer indicated formation of crystalline domains which appeared to be in perfect register with solid domains of the DMPE monolayer. This led to the conclusion that quasi-crystalline domains were formed in the DMPC monolayer exactly

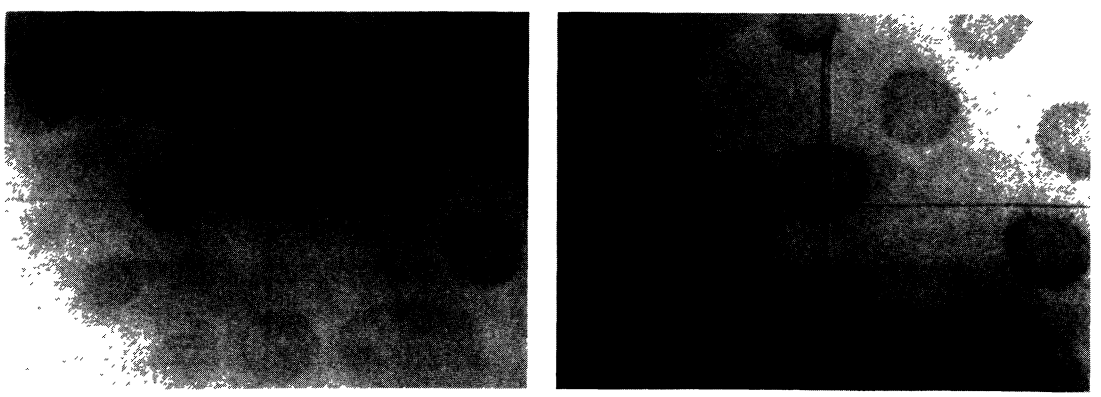

Fig. 6. — Fluorescence micrographs of a supported bilayer with the proximal monolayer being DMPE doped with 1 % Texas-Red DMPE (deposited at 14 mN/m at 30 °C) and the distal monolayer being DMPC doped with 1 % NBD-DMPE (deposited from 20 mN/m at 30 °C). Left side : excitation of NBD at 465 nm. Right side : excitation of Texas-Red at 596 nm. Note the complete register of the dark domains. Length of the upper doubled bar is 60 μm.

opposite the crystalline domains in the DMPE layer. Evidence of similar epitactic monolayer-coupling was found by Tamm and McConnell [19]. These investigators discovered that epitactic effects caused fluid and solid domains in the monolayers to be coincident if both were deposited from a state of coexistence.

4.2 FRUSTRATED PHASE TRANSITIONS IN SUBSTRATE COUPLED BILAYERS. — It has been pointed out previously [7, 20] that low pressure condensed phases ($\pi < \pi_c$) are crystalline but include a high density of defects. These defects were considered to be responsible for the mechanical softness observed in condensed platelets. The high defect density was attributed to incommensurability of the lattices preferred by the chains (triangular) vis a vis the head groups (orthorhombic). In addition to this frustration, phase transitions in supported bilayers were further impeded by total area constraints. Area constraints were less restrictive if proximal layers were decoupled from the surface by a water film since the bilayers could buckle into the third dimension during expansion which led to formation of blobs protruding from the bilayer.

In the case of fixed proximal layers (e.g. DMPC in Fig. 3), transition from the fluid to solid state in the distal layer must have occurred through either chain tilting (such as in a smectic A to smectic C-transition) or interdigitation of the cahins (cf. Fig. 7) without expansion of area. In the former case, it is expected that formation of a whole network of Néel- or Bloch-like walls would enable fast long-range diffusion even in the solid phase. Ample evidence for this has been found in the $P_{\beta'}$-phase of vesicles [21, 22]. The diffusion has been attributed to a percolation process [23]. In this situation, the reduction observed in the diffusion coefficient can no longer be simply related to a viscous drag between monolayers. Of the two types of structural changes (tilting or interdigitation) at phase transitions, we favor interdigitation as the mechanism for the case of DMPC on HTS. This was suggested by the remarkable finding (Fig. 3b) that the diffusion coefficient increased with increasing surface density in the distal monolayer *and* because (at a specific transfer pressure for the distal monolayer, e.g. 20 dyn/cm, Fig. 3b), diffusivity was reduced when the packing density (or transfer pressure) of the proximal monolayer was decreased (compare curves for $\pi_d = 17$ and 20 dyn/cm). These features were consistent with interpenetration of the chains between monolayers to attain optimal packing of the central hydrocarbon region. As a consequence, it was expected that interdigitation would increase as the difference between packing densities of the proximal and distal monolayers increased.

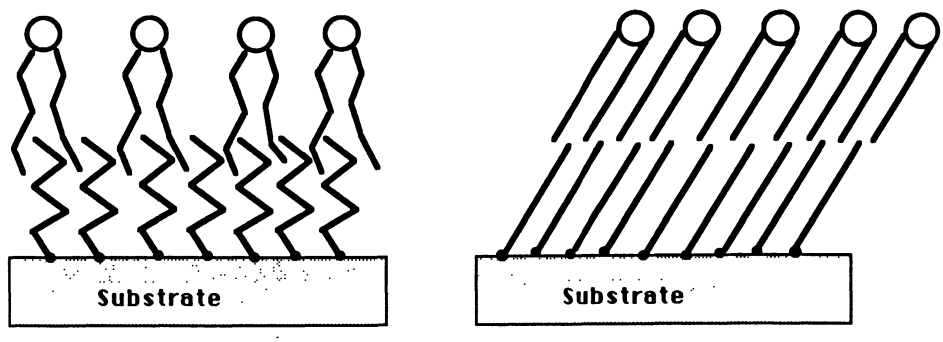

Fig. 7. — Two possibilities of the crystallization of supported bilayers with fixed total area. Left : intercalation of chains. Right : collective tilting of chains (in analogy to smectic A-to-smectic C transitions).

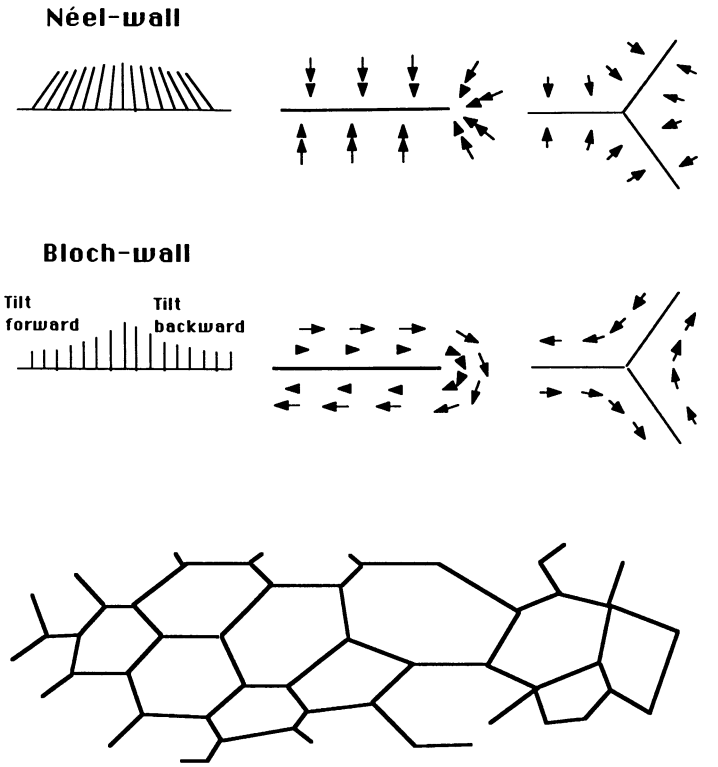

Fig. 8. — Schematic representation of Bloch and Néel walls and of a network of interconnected walls allowing for short circuit diffusion over long distances. Note that the number of defects lines can easily decrease by attraction and cancellation.

For situations where the fluorescence recovery was high (e.g. $> 80\ \%$) representative of fluid layers, crystalline domains (if present) were so small that monolayers could be considered as quasi-continuous fluids. For example, both above and below the conformational transitions observed in some tests of DMPC on fixed silane monolayers, nearly complete recovery was exhibited by probes in the distal layer and the diffusivity decreased continuously with temperature (e.g. Figs. 3a and c). Similar levels of recovery were obtained for all tests of DOPC on fixed silane monolayers (Fig. 2). In these tests, fluorescence micrographs also showed uniform fluorescence patterns over the whole temperature range. Consequently, the model for viscous coupling between a fluid monolayer and a substrate could be used to analyze the effects of substrate drag on the mobility of probes in the distal layer. Here again, it was expected that viscous drag between monolayers would increase as interdigitation increased. However, chain interpenetration was unlikely in the case of DOPC on Cd-arachidate. Here, the proximal monolayer was in a tightly-packed crystalline state (at 30 dyn/cm transfer pressure).

5. Concluding discussion.

Diffusion measurements in supported bilayers together with the fluid mechanical theory for particle mobility [1] provides a powerful tool for studying viscous friction between monolayers

and between lipid layers and substrates. When the interfacial drag is high ($\varepsilon > 1$), the diffusion coefficient becomes strongly dependent on the particle radius ($D \propto a_p^{-2}$) which opens-up new possibilities to estimate radii of surface molecules, e.g. macromolecular lipids. This regime is easily attained by fixing the proximal layer to the substrate as demonstrated by DOPC on Cd-arachidate. However, to improve reliability in the analysis of such measurements, separate determination of the two-dimensional monolayer viscosity is necessary or calibration with probes of known dimension. As shown in the present work, the viscous friction exerted by one monolayer against another depends on the surface packing density, substrate-monolayer rigidity, and the degree of interdigitation between the hydrocarbon chains of adjacent layers. For example, comparison of experiments with DOPC on Cd-arachidate and silanes showed that the viscous friction coefficient for a fluid monolayer adjacent to a fixed crystalline layer (Cd-arachidate) was by 10-50 times greater than for a fluid monolayer next to a proximal layer in the fluid state (HTS or OTS). Further, large differences in viscous friction coefficients were found for liquid-on-liquid chains which appeared to be determined by interdigitation of hydrocarbon chains.

Another important (perhaps biologically relevant) aspect is the potentially large viscous drag that can be created by friction between a substrate and proximal monolayer. Such effects suggest that the coupling between a plasma membrane bilayer and the subsurface cytoskeleton in cell membranes may impede lateral diffusion of proteins embedded in the bilayer even in the absence of direct covalent protein/cytoskeletal anchorage. For instance, the immobilization of Band III in erythrocytes may well be due to viscous interfacial drag [24]. In particular, we have found that strong monolayer/substrate coupling can reduce lateral mobility in bilayers on glass by several orders of magnitude if the glass was not pre-treated by Argon sputtering to produce a lubricating water film between the proximal monolayer and the substrate.

References

[1] EVANS E. and SACKMANN E., *J. Fluid Mech.* **194** (1988) 553.
[2] STELZLE M. and SACKMANN E., accepted for publication in BBA.
[3] TURNER A. P. F., KARUBA I. and WILSON G. S., Biosensors Fundamentals and Applications (Oxford University Press) 1987.
[4] WATTS T. H., GAUB H. and MCCONNELL H. M., *Nature London* **320** (1986) 179-181.
[5] SCHNEIDER G., KNOLL W., SACKMANN E., JOOSTEN J. G. H., *Europhys. Lett.* **1** (1986) 449.
[6] RUBINSTEIN I., STEINBERG S., TOR Y., SHANCER A. and NAGIV J., *Nature* **332** (1988) 426-429.
[7] FISCHER A. and SACKMANN E., *J. Phys. France* **45** (1984) 517.
[8] MCCONNELL H. M. and TAMM L. K., *Biophys. J.* **47** (1985) 105.
[9] GAUB H., BÜSCHL R., RINGSDORF H. and SACKMANN E., *Biophys. J.* **45** (1984) 725.
[10] AXELROD D., KOPPEL D. E., SCHLESSINGER J., ELSON E. L. and WEBB W. W., *Biophysics J.* **16** (1976) 1055.
[11] GALLA H. J., HARTMANN W., THEILEN U. and SACKMANN E., *J. Membr. Biol.* **48** (1979) 215.
[12] VAZ W. L. C., CLEGG R. M. and HALLMANN D., *Biochemistry* **24** (1985) 781.
[13] SEUL M. and MCCONNELL H. M., *J. Phys. France* **47** (1986) 1587-1604.
[14] SAFFMANN P. G. and DELBRÜCK M., *Proc. Natl. Acad. Sci. USA* **72** (1975) 3111.
[15] HUGHES G. D., PAILTHORPE B. A., WHITE L. R. and SAWYER W. H., *J. Fluid Mech.* **110** (1981) 349.
[16] PETERS R. and BECK K., *Proc. Natl. Acad Sci. USA* **72** (1983) 7183.
[17] EVANS E. E. and SKALAK R., Mechanics and Thermodynamics of Biomembranes (CRC Press, Boca Raton, Florida), 1980.

[18] NAGLE J., *Faraday Discuss.* **81** (1986).
[19] MCCONNELL H. M., TAMM L. K. and WEIS R. M., *Proc. Natl. Acad. Sci. USA* **81** (1984) 3249.
[20] SACKMANN E., FISCHER A. and FREY W., Physics of Amphiphilic Layers, Eds. J. Meunier, D. Langevin and N. Boccara, *Springer Proc. Phys.* (Springer, Berlin Heidelberg) **21** (1987) 21.
[21] KAPITZA H. G., RÜPPEL D. A., GALLA H. J. and SACKMANN E. *Biophys. J.* **45** (1984) 577-587.
[22] SCHNEIDER M. B. and WEBB W. W., *J. Phys. France* **45** (1984) 273-281.
[23] SAXTON M. J., *Biophys. J.* **52** (1987) 989-997.
[24] CHERRY R. J. and GODFREY R. E., *Biophys. J.* **36** (1981) 257-276.